Mixed-Addenda Vanadium-Substituted Polyfluorooxometalates: Synthesis, Characterization, and Catalytic Aerobic Oxidation

Alexander M. Khenkin and Ronny Neumann*

Department of Organic Chemistry, Weizmann Institute of Science, Rehovot 76100, Israel

Received May 25, 1999

For the first time, mixed-addenda vanadium-substituted polyfluorooxometalates, PFOMs, have been synthesized. Depending on the workup procedure used, two types of compounds were prepared. The first PFOM was a quasi Wells−Dawson type compound, $[H_2F_6NaV^{V}W_{17}O_{56}]^{8-}$, and the second a mixture of vanadium-substituted polyfluorooxometalates of the Keggin structure, $XV^{IV}W_{11}F_nO_{40-n}$ (X = H_2, V, W; $n = 1-4$). From the X-ray diffraction analysis, $[H_2F_6NaV^{V}W_{17}O_{56}]^{8-}$ has an elliptic (egg) shape with a central sodium atom surrounded by six fluorine atoms in a trigonal prism coordination. One may differentiate between two types of addenda atoms to be found in belt and capped positions. According to ^{1}H, ^{19}F, and ^{51}V NMR analysis, it is concluded that vanadium is isomorphically substituted in both the belt and capped position of $[H_2F_6NaV^{V}W_{17}O_{56}]^{8-}$. The mixture of vanadium-substituted PFOMs of the Keggin structure was shown, by HPLC and ESR, to contain at least two species of different charge and of a different vanadium environment. The $[H_2F_6NaV^{V}W_{17}O_{56}]^{8-}$ PFOM was active for the catalytic aerobic oxidation of alkyl aromatic compounds in biphasic (water-catalyst and substrate) media. The reaction selectivity (autoxidation versus oxydehydrogenation) depended on the substrate and reaction conditions such as temperature and oxygen pressure. The selectivity to oxydehydrogenation was significantly higher compared to the prototypical cobalt acetate catalytic system.

Introduction

Polyoxometalates have very significant potential as practical oxidation catalysts[1] due to their inherent stability to strongly oxidizing conditions and the possibility of activation of environmentally and economically favored oxidants such as molecular oxygen and hydrogen peroxide. Interestingly, despite the fact that many different structures have been identified and a structure−catalytic activity relationship may be expected, most research in the area of catalytic oxidation has been carried out on relatively few polyoxometalate compounds. Especially notable have been the iron-,[2] manganese-,[3] and ruthenium-substituted[4] Keggin- and "sandwich"-type tungsten-based structures and the mixed-addenda Keggin-type vanadomolybdate, $PV_2Mo_{10}O_{40}^{5-}$.[5] Common to these catalysts has been the exclusive metal−oxide nature of these compounds. It has on occasion been shown in the past that some of the oxygen positions in polyoxometalates can be replaced by sulfur[6] or fluorine atoms.[7] Partial substitution of an oxide position by fluoride, for example, might be expected to have a significant electronic effect on a neighboring transition metal center, leading to a change in or new catalytic activity. The synthesis of *non* transition metal substituted polyfluorooxometalates, PFOMs, of both the Keggin structure and of a more elongated elliptic structure akin to Wells−Dawson type polyoxometalates (herein termed quasi Wells−Dawson) has led to quite well-defined compounds.[7] On the other hand, transition metal substituted PFOMs of the Keggin type, predictably derived from lacunary parent species, are less well-characterized since the synthesis

(1) (a) Hill, C. L.; Prosser-McCartha, C. M. *Coord. Chem. Rev.* **1995**, *143*, 407. (b) Okuhara, T.; Mizuno, N.; Misono, M. *Adv. Catal*. **1996**, *41*, 113I. (c) Neumann, R. *Prog. Inorg. Chem.* **1998**, *47*, 317. (d) Kozhevnikov, I. V. *Chem. Rev.* **1998**, *98*, 171.

(2) (a) Khenkin, A. M.; Hill, C. L. *Mendeleev Commun.* **1993**, 140. (b) Zhang, X.; Chen, Q.; Duncan, D. C.; Lachicotte, R. J.; Hill, C. L. *Inorg. Chem.* **1997**, *36*, 4381. (c) Zhang, X.; Chen, Q.; Duncan, D. C.; Campana, C. F.; Hill, C. L. *Inorg. Chem.* **1997**, *36*, 4208. (d) Mizuno, N.; Hirose, T.; Tateishi, M.; Iwamoto, M. *J. Mol. Catal*. **1994**, *88*, L125. (e) Mizuno, N.; Tateishi, M.; Hirose, T.; Iwamoto, M. *Chem. Lett*. **1993**, 2137. (f) Mizuno, N.; Nozaki, C.; Kiyoto, I.; Misono, M. *J. Am. Chem. Soc.* **1998**, *120*, 9267. (g) Mizuno, N.; Kiyoto, I.; Nozaki, C.; Misono, M. *J. Catal*. **1999**, *181*, 171.

(3) (a) Neumann, R.; Gara, M. *J. Am. Chem. Soc.* **1994**, *116*, 5509. (b) Neumann, R.; Gara, M. *J. Am. Chem. Soc*. **1995**, *117*, 5066. (c) Neumann, R.; Juwiler, D. *Tetrahedron* **1996**, *47*, 8781. (d) Neumann, R.; Khenkin, A. M.; Juwiler, D.; Miller. H.; Gara, M. *J. Mol. Catal.* **1997**, *117*, 169. (e) Neumann, R.; Khenkin, A. M. *Chem. Commun.* **1998**, 1967. (f) Bösing, M.; Nöh, A.; Loose, I.; Krebs, B. *J. Am. Chem. Soc.* **1998**, *120*, 7252. (g) Mansuy, D.; Bartoli, J.-F.; Battioni, P.; Lyon, D. K.; Finke, R. G. *J. Am. Chem. Soc.* **1991**, *113*, 7222. (h) Zhang, X.-Y.; Pope, M. T. *J. Mol. Catal. A: Chem*. **1996**, *114*, 201.

(4) (a) Neumann, R.; Dahan, M. *J. Chem. Soc., Chem. Commun.* **1995**, 171. (b) Neumann, R.; Khenkin, A. M.; Dahan, M. *Angew. Chem., Int. Ed. Engl.* **1995**, *34*, 1587. (c) Neumann, R.; Dahan, M. *Nature* **1997**, *388*, 353. (d) Neumann, R.; Dahan, M. *Polyhedron* **1998**, *17*, 3557. (e) Neumann, R.; Dahan, M. *J. Am. Chem. Soc.* **1998**, *120*, 11969. (f) Neumann, R.; Khenkin, A. M. *Inorg. Chem.* **1995**, *34*, 5753. (g) Neumann, R.; Abu-Gnim, C. *J. Am. Chem. Soc.* **1990**, *112*, 6025.

(5) (a) K. I. Matveev, K. I. *Kinet. Catal.* **1977**, *18*, 716. (b) Grate, J. R.; Mamm, D. R.; Mohajan, S. *Mol. Eng.* **1993**, *3*, 205. (c) Neumann, R.; Assael, I. *J. Chem. Soc., Chem. Commun.* **1988**, 1285. (d) Gall, R. D.; Faraj, M.; Hill, C. L. *Inorg. Chem.* **1994**, *33*, 5015. (e) Neumann, R.; Levin, M. *J. Org. Chem.* **1991**, *56*, 5707. (f) Neumann, R.; Lissel, M. *J. Org. Chem.* **1989**, *54*, 4607. (g) Kholdeeva, O. A.; Golovin, A. V.; Maksimovskaya, R. A.; Kozhevnikov, I. V. *J. Mol. Catal.* **1992**, *75*, 235. (h) Lissel, M.; Jansen van de Wal, H.; Neumann, R. *Tetrahedron Lett.* **1992**, *33*, 1795. (i) Neumann, R.; Levin, M. *J. Am. Chem. Soc.* **1992**, *114*, 7278. (j) Khenkin, A. M.; Rosenberger, A.; Neumann, R. *J. Catal.* **1999**, *182*, 82.

(6) Cadot, E.; Bereau, V.; Marg, B.; Halut, S.; Secheresse, F. *Inorg. Chem.* **1996**, *35*, 3099.

(7) (a) Chauveau, F.; Souchay, P. *J. Inorg. Nucl. Chem.* **1974**, *36*, 1761. (b) Launay, J.-P.; Boyer, M.; Chauveau, F. *J. Inorg. Nucl. Chem.* **1976**, *38*, 243. (c) Chauveau, F.; Doppelt, P.; Lefebvre, J. *Inorg. Chem.* **1980**, *19*, 2803. (d) Jorris, T. L.; Kozik, M.; Baker, L. C. W. *Inorg. Chem.* **1990**, *29*, 4584.

10.1021/ic990606s CCC: $19.00
Published on Web 07/12/2000

Scheme 1

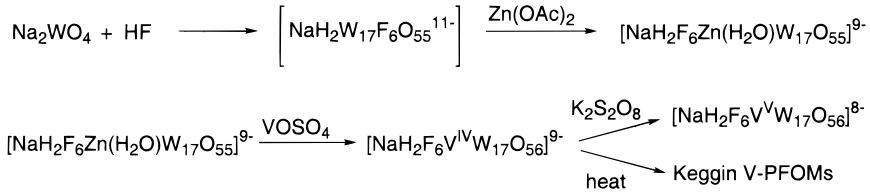

with a specified number and position of the fluorine atoms is not easily planned and/or rationalized.[8] There is, on the other hand, an example of partially characterized iron- and cobalt-substituted PFOMs, $[M(H_2O)H_2F_6NaW_{17}O_{55}]^{9-}$ (M = Co, Fe),[9] of the quasi Wells−Dawson structure.

Despite the importance of vanadium-based compounds in oxidation catalysis, and the wide use, as catalysts, of mixed-addenda vanadium-substituted polyoxometalates, vanadium-substituted polyfluorooxometalates have to date neither been prepared, characterized, nor used as catalysts. Therefore, we have undertaken to study and now report on the synthesis and characterization of mixed-addenda vanadium-substituted polyfluorooxometalates, PFOMs. Furthermore, we describe for the first time the use of polyfluorooxometalates in oxidation catalysis, specifically the aerobic autoxidation and oxydehydrogenation of alkylaromatic compounds.

Results and Discussion

Synthesis of Vanadium-Substituted PFOMs. In order to prepare vanadium-substituted PFOMs, Scheme 1, the $[Zn(H_2O)H_2F_6NaW_{17}O_{55}]^{9-}$ PFOM was used as starting material. The zinc-substituted PFOM was resynthesized according to Jorris.[10] Accordingly, a lacunary PFOM was prepared in situ by reacting sodium tungstate with 49% HF until the pH reached 4.5. The white precipitate, of unknown composition, formed was removed by filtration. Zinc acetate was added to the filtrate containing the lacunary PFOM, yielding the desired zinc-substituted PFOM, $[Zn(H_2O)H_2F_6NaW_{17}O_{55}]^{9-}$. From the X-ray structure of the analogous vanadium-substituted product presented below, Figure 1, there are two possible types of tungsten (zinc) positions: a capped position and a belt position. Based on this crystalline starting material metathetical exchange of the zinc transition metal applying the method used for vanadium-substituted "sandwich"-type compounds[11] was carried out using 2 equiv of $V^{IV}OSO_4$. The metathetical exchange occurred almost immediately, and a dark purple precipitate tentatively formulated as the mixed-addenda PFOM, $[H_2F_6NaV^{IV}W_{17}O_{56}]^{9-}$, was obtained. This initial precipitate was treated in two ways. First, after dissolution, the vanadium (IV), $[H_2F_6NaV^{IV}W_{17}O_{56}]^{9-}$, was oxidized using peroxydisulfate to yield $[H_2F_6NaV^{V}W_{17}O_{56}]^{8-}$, which was reisolated and recrystallized from hot water. Only yellow *needlelike* single crystals entirely representative of the bulk sample were obtained. Characterization (see below) showed that indeed the quasi Wells−Dawson compound, $[H_2F_6NaV^{V}W_{17}O_{56}]^{8-}$, was obtained. The second treatment, direct recrystallization of the initially formed $[H_2F_6NaV^{IV}W_{17}O_{56}]^{9-}$ from boiling water without first carrying out peroxydisulfate oxidation, yielded purple-black *cubic* crystals. Characterization (see below) of these crystals showed them to be a *mixture* of vanadium-substituted Keggin-type PFOMs, tentatively formulated as $XV^{IV}W_{11}F_nO_{40-n}$ (X = H_2, V, W; $n = 1-4$). We were unable to separate the mixture by crystallization. These Keggin-type PFOMs could also be oxidized with $K_2S_2O_8$ to analogous vanadium(V) species and further characterized.

Since the oxidized $[H_2F_6NaV^{V}W_{17}O_{56}]^{8-}$ could more easily be recrystallized from hot water while the reduced $[H_2F_6NaV^{IV}W_{17}O_{56}]^{9-}$ rearranged to a mixture of Keggin-type structures upon heating, one may conclude that the oxidized form is significantly more stable than the reduced species. One can further surmise that the Keggin structure is apparently thermodyamically more stable compared to the quasi Wells−Dawson structure for the V^{IV} PFOM-type compounds. Assuming as for other vanadium-substituted polyoxometalates[11] that decomposition begins by disassociation at a vanadium-substituted position, one can logically speculate that according to eq 1 $K_1 > K_2$ and/or $k_1 > k_2$. This is because (a) the 11− lacunary compound should be less stable compared to the 9− lacunary species and will further decompose once formed and (b) the disassociation of VO_2^+ is less likely than that of VO^{2+} [12] because a greater perturbation in structure is necessary, requiring

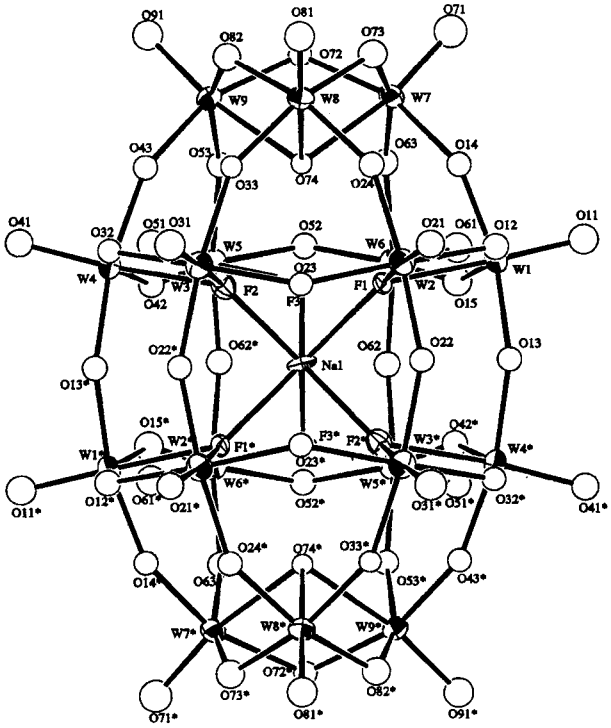

Figure 1. ORTEP view of $[H_2F_6NaV^{V}W_{17}O_{56}]^{8-}$.

(8) (a) Wasfi, S. H.; Johnson, W. L.; Martin, D. L. *Synth. React. Inorg. Met.* **1997**, *27*, 401. (b) Wasfi, S. H.; Johnson, J. C. *Synth. React. Inorg. Met.* **1996**, *26*, 1073. (c) Wasfi, S. H.; Johnson, J. C. *Synth. React. Inorg. Met.* **1996**, *26*, 1339. (d) Wasfi, S. H.; Johnson, J. C.; Martin, D. L. *Synth. React. Inorg. Met.* **1995**, *26*, 1061. (e) Wasfi, S. H.; Johnson, W. L.; Martin, D. L. *Inorg. Chim. Acta* **1998**, *278*, 91. (f) Wasfi, S. H.; Johnson, W. L.; Martin, D. L. *Synth. React. Inorg. Met.* **1997**, *27*, 535. (g) Wasfi, S. H.; Rheingold, A. L.; Haggerty, B. S. *Inorg. Chim. Acta* **1998**, *282*, 136.

(9) Wasfi, S. H.; Costello, C. E.; Rheingold, A. L.; Haggerty, B. S. *Inorg. Chem.* **1991**, *30*, 1788.

(10) Jorris, T. L. Ph.D. Thesis, Georgetown University, 1987.

(11) Tourné, C. M.; Tourné, G. F.; Zonnevijlle, F. *J. Chem. Soc., Dalton Trans.* **1991**, 143.

Table 1. Crystallographic Data for $K_8[H_2F_6NaVW_{17}O_{56}]\cdot 7H_2O$

space group	*C*2/*c*
a, Å	22.736(3)
b, Å	12.335(2)
c, Å	29.504(5)
β, deg	92.15(2)
V, Å^3	8269(2)
z	4
ρ_{calcd}, g cm^{-3}	3.83
μ(Mo Kα), cm^{-1}	239.92
no. of unique reflns	7648
no. of reflns with $I \geq 3\sigma_I$	4775
R (R_w)	0.050 (0.069)

Table 2. Selected Bond Distances (Å) and Bond Angles (deg) in $[H_2F_6NaV^VW_{17}O_{56}]^{8-}$

Bond Distances

belt position		capped position	
W(1)−F(1)	2.21(1)	W(7)−O(14)	1.97(2)
W(1)−O(11)	1.68(2)	W(7)−O(63)	1.87(2)
W(1)−O(12)	1.92(2)	W(7)−O(71)	1.71(2)
W(1)−O(13)	1.90(2)	W(7)−O(72)	1.94(2)
W(1)−O(14)	1.87(2)	W(7)−O(73)	1.95(2)
W(1)−O(15)	1.91(2)	W(7)−O(74)	2.26(2)

Bond Angles

belt position		capped position	
F(1)−W(1)−O(11)	172.1(8)	O(14)−W(7)−O(63)	88.4(8)
F(1)−W(1)−O(12)	72.9(7)	O(14)−W(7)−O(71)	102.9(9)
F(1)−W(1)−O(13)	84.1(7)	O(14)−W(7)−O(72)	159.2(7)
F(1)−W(1)−O(14)	83.3(7)	O(14)−W(7)−O(73)	87.9(8)
F(1)−W(1)−O(15)	84.6(7)	O(14)−W(7)−O(74)	85.6(7)
O(11)−W(1)−O(12)	99.3(9)	O(63)−W(7)−O(71)	102(1)
O(11)−W(1)−O(13)	96.4(9)	O(63)−W(7)−O(72)	88.1(8)
O(11)−W(1)−O(14)	96.5(9)	O(63)−W(7)−O(73)	159.7(8)
O(11)−W(1)−O(15)	103.3(9)	O(63)−W(7)−O(74)	86.4(7)
O(12)−W(1)−O(13)	89.6(8)	O(71)−W(7)−O(72)	97.8(9)
O(12)−W(1)−O(14)	89.5(8)	O(71)−W(7)−O(73)	98(1)
O(12)−W(1)−O(15)	157.4(8)	O(71)−W(7)−O(74)	168.2(8)
O(13)−W(1)−O(14)	167.0(7)	O(72)−W(7)−O(73)	88.3(8)
O(13)−W(1)−O(15)	87.9(8)	O(72)−W(7)−O(74)	73.8(7)
O(14)−W(1)−O(15)	87.9(8)	O(73)−W(7)−O(74)	73.4(7)

more energy, to remove both bridging and terminal oxygen atoms of the PFOM structure in the case of the oxidized species.

$$[NaH_2F_6V^{IV}W_{17}O_{56}]^{9-} \underset{}{\overset{K_1}{\rightleftharpoons}} VO^{2+} + [NaH_2F_6W_{17}O_{55}]^{11-}$$
$$[NaH_2F_6V^{V}W_{17}O_{56}]^{8-} \underset{}{\overset{K_2}{\rightleftharpoons}} VO_2^{+} + [NaH_2F_6W_{17}O_{54}]^{9-} \quad (1)$$

Characterization of the Quasi Wells−Dawson $[H_2F_6NaVW_{17}O_{56}]^{q-}$. The structure of the potassium salt, $K_8H_2F_6NaV^VW_{17}O_{56}\cdot 7H_2O$, Figure 1 and Table 1, was determined by X-ray crystallography. Selected bond lengths and angles, Table 2 (a total listing of positional parameters, intramolecular distances, and intramolecular bond angles is available as Supporting Information), show that $[H_2F_6NaV^VW_{17}O_{56}]^{8-}$ is isostructural to the $[H_2F_6NaW_{18}O_{56}]^{7-}$ anion reported previously.[7c,d,9] There is a central core consisting of a sodium atom surrounded by six crystallographically identical fluorine atoms (distance 2.22−2.26 Å) in a triganol prism coordination. It was not possible to resolve the position of the one vanadium atom among the remaining 17 tungsten atoms, nor could one determine if vanadium was exclusively in a belt or capped position. The 12 tungsten (vanadium) atoms in the belt positions have a distorted octahedral (tetragonal) coordination, with

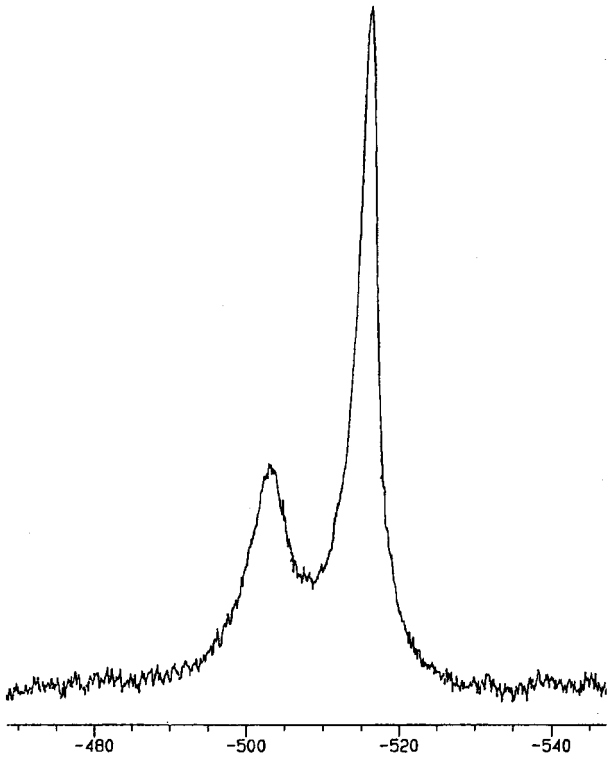

Figure 2. ^{51}V NMR of $K_8[H_2F_6NaV^VW_{17}O_{56}]$ in D_2O.

W(V)−O bond lengths of ∼1.9 Å for the bridging oxygen positions, W(V)−O bond lengths of ∼1.7 Å for the terminal oxygen positions, and longer W(V)−F bonds, 2.2 Å. The six tungsten (vanadium) atoms in the capped position have a very similar tetragonal coordination with W(V)−O bond lengths of ∼1.9 Å for the bridging oxygen positions, W(V)−O bond lengths of ∼1.7 Å for the terminal oxygen positions, and longer W(V)−O74 bonds, ∼2.2 Å. The position of the hydrogen atoms was not resolved in the X-ray structure, but is surmised to be between the O74 oxygen and F1, F2, and F3 forming F_3HO tetrahedra (see the ^{1}H NMR spectrum, Figure 5).

The ^{51}V NMR spectrum of $K_8H_2F_6NaV^VW_{17}O_{56}$ in D_2O is shown in Figure 2. Two peaks at −502 and −516 ppm (referenced to $VOCl_3$; $\Delta\nu_{1/2}$ = 490 and 270 Hz, respectively) are observed with an area ratio of ∼1:1.75. The peaks are slightly downfield shifted compared to those of other monovanadotungstates.[13] It is enticing to say that since the X-ray crystal structure shows 6 end-capped tungsten (vanadium) atoms and 12 belt tungsten (vanadium) positions, equal (statistical) and isomorphous substitution of one vanadium atom would be expected to give, approximately, the observed peak areas. Additionally, since proximate fluorine substitution in the belt position would be expected to give an upfield shift in the ^{51}V NMR, the relative shifts of the peaks are logical. For example, for VO_4^{3-}, $\delta = -540$ ppm; for $VO_2F_2^{1-}$, $\delta = -595$ ppm; and for VOF_4^{1-}, $\delta = -797$ ppm.[14] The relative peak areas (capped and belt) correlate with the chemical shift. Attempts to separate the two isomers by crystallization were not successful. Furthermore, the ^{51}V NMR spectrum showed the formation of both isomers upon addition of even a substoichiometric amount, 0.25 and 0.5 equiv of vanadium sulfate, to the initial zinc compound. The probable existence of equilibrium reactions as described in eq 1 underlines the likelihood of finding vanadium in both the belt and capped positions.

(12) Bayer, R.; Marchal,-Roch, C.; Liu, F. X.; Tézé, A.; Hervé, G. *J. Mol. Catal.* **1996**, *110*, 65.
(13) Leparulo-Loftus, M. A.; Pope, M. T. *Inorg. Chem.* **1987**, *26*, 2112.
(14) Hibbert, R. C. *J. Chem. Soc., Dalton Trans.* **1986**, 751.

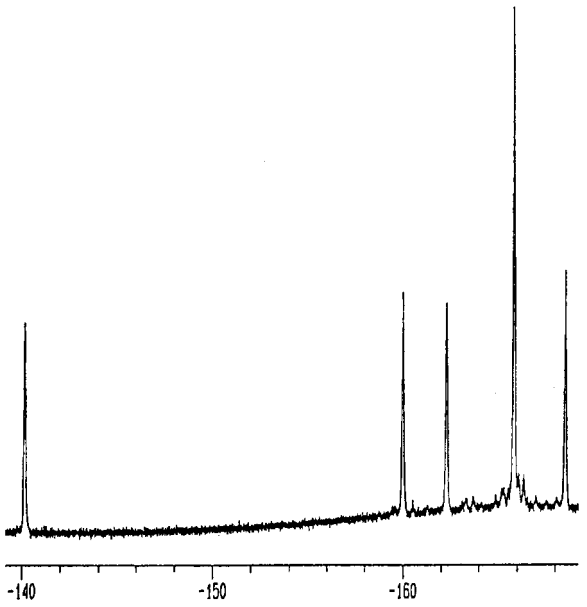

Figure 3. ^{19}F NMR of $K_8[H_2F_6NaVW_{17}O_{56}]$ in D_2O.

The ^{19}F NMR spectrum (CF_3COOH as reference) of $K_8H_2F_6NaV^VW_{17}O_{56}$ in D_2O, Figure 3, reveals the complexity of the NMR spectrum for the mixture of two vanadium positional isomers. Five peaks are observed at −140.17 (1), −159.96 (1.2), −162.26 (1.2), −165.82 (2.8), and −168.50 (1.2) ppm (intensity). Substitution of one vanadium atom in place of a tungsten atom reduces the symmetry of the PFOM and leads to new peaks. Theoretically, vanadium substitution into a belt position only would be expected to yield a six-line ^{19}F NMR spectrum with peaks of equal intensity. On the other hand substitution in a capped position only would be expected to show a four-line ^{19}F NMR spectrum of a 1:1:1:3 intensity ratio (assuming the three fluorine atoms distal to vanadium in a capped position are NMR equivalent). Considering a theoretical 2:1 ratio of belt versus capped positions, all in all 10 lines might be expected with an area ratio of 2:2:2:2:2:2:1:1:1:3. Clearly, the expected spectrum was not obtained; rather a five-line spectrum of ∼1:1:1:2.5:1 was measured. From the literature[10] it was claimed for the analogous zinc-substituted compound, which was the starting material for the present $[H_2F_6NaV^VW_{17}O_{56}]^{8-}$ synthesis, that the zinc is exclusively found in the belt position. Thus, the observed five line spectrum was explained by the coalescence of two of the six expected lines, yielding a five-line spectrum (1:1:1:2:1) peak intensity. We were skeptical about this conclusion for three major reasons. First, the chemical shifts were spread over a rather wide range. From the X-ray data, in the case of the placement of the vanadium atom in a belt position the atom distance from the proximate fluorine is ∼2.21 Å, while other V−F distances are 3.94, 4.06, 5.05, 5.15, and 6.01 Å. A wide range of chemical shifts was not expected considering the large interatomic distances. Notably, vanadium in a capped position also yields V−F interatomic distances ranging between 3.96 and 6.6 Å. Second, the spectrum was not affected by the identity of the substituted metal. The same spectra, within experimental error, were observed for the zinc- and vanadium-substituted compounds. Third, often in vanadium-substituted polyoxometalates, for example, the extensively studied $PV_2Mo_{10}O_{40}^{5-}$, there is fast exchange of the vanadium positions in *aqueous* solutions on the NMR time scale. This prevents, for example, complete ^{31}P NMR spectral resolution in water. One way to overcome this problem and to obtain higher resolution, utilizing the limited solubility of VO_2^+ in organic media, is to carry out the measurements in an organic solvents such as acetonitrile.[5i,j] Thus, $K_8H_2F_6NaV^VW_{17}O_{56}$ was treated with an excess of $(C_4H_9)_4NBr$ to form, by metathetical exchange of the cation, $Q_8H_2F_6NaV^VW_{17}O_{56}$ ($Q = (C_4H_9)_4N^+$), which is the soluble in acetonitrile. The ^{51}V NMR spectrum of $Q_8H_2F_6NaV^VW_{17}O_{56}$ in CD_3CN was similar to the spectrum of $K_8H_2F_6NaV^VW_{17}O_{56}$ in D_2O, with however poorer resoltion of the peaks and an upfield shift of the peaks to −562 and −579 ppm. The ^{19}F NMR of $Q_8H_2F_6NaV^VW_{17}O_{56}$ in CD_3CN, Figure 4, on the other hand shows an entirely different spectrum exhibiting a different number of peaks, a different ratio of peak intensities, and a much narrower range of chemical shifts, between −161 and −168 ppm. There are five major peaks (two shoulders marked by arrows) between −164 and −166 ppm. Very notable is also the disappearance of the peak downfield at −140 ppm. None of the peaks are attributable to F−H coupling as the spectrum was unchanged by ^1H decoupling. Although neither the number of peaks nor their relative intensity allowed the determination of the exact distribution of the vanadium atom between the two possible isomers, the spectrum does definitely discount the possibility of substitution in the belt or capped position only. The observation that the peak at −140 ppm found in D_2O was not measured in CD_3CN quite conceivably could mean that that peak may be associated with a lacunary species.

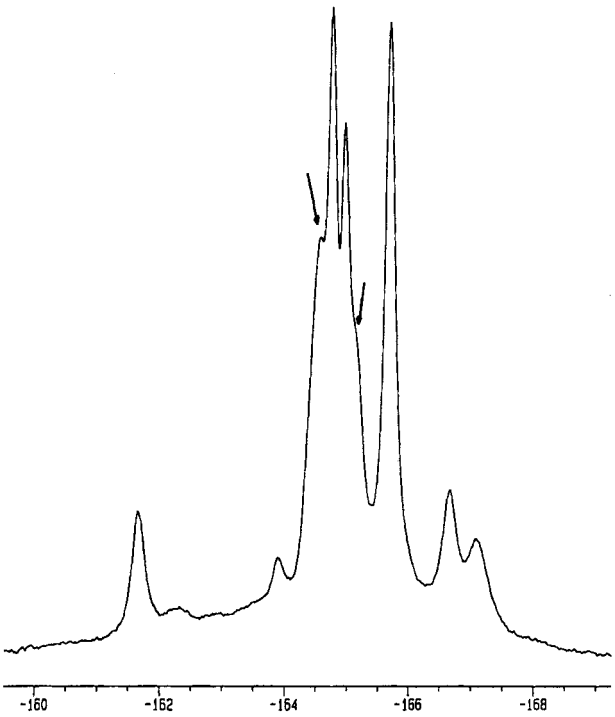

Figure 4. ^{19}F NMR of $Q_8[H_2F_6NaVW_{17}O_{56}]$ in CD_3CN.

The $Q_8H_2F_6NaV^VW_{17}O_{56}$ compound dissolved in CD_3CN was further used to probe the chemical environment of the hydrogen atoms in the central core.[15] The ^{19}F-decoupled ^1H NMR of $[H_2F_6NaV^VW_{17}O_{56}]^{8-}$, Figure 5, bottom, shows four peaks at 5.09, 4.97, 4.91, and 4.77 ppm with area ratio of 1.6:1.6:1.1:1.0. There is an additional peak at 4.84 ppm which is associated with an impurity (2.5% by integration) and two additional impurities (not shown), <1% each, at 5.41 and 4.62 ppm. Thus, this ^1H NMR is also an effective measure of the

(15) It is difficult to measure the ^1H NMR spectrum in D_2O due to interference from HOD impurities.

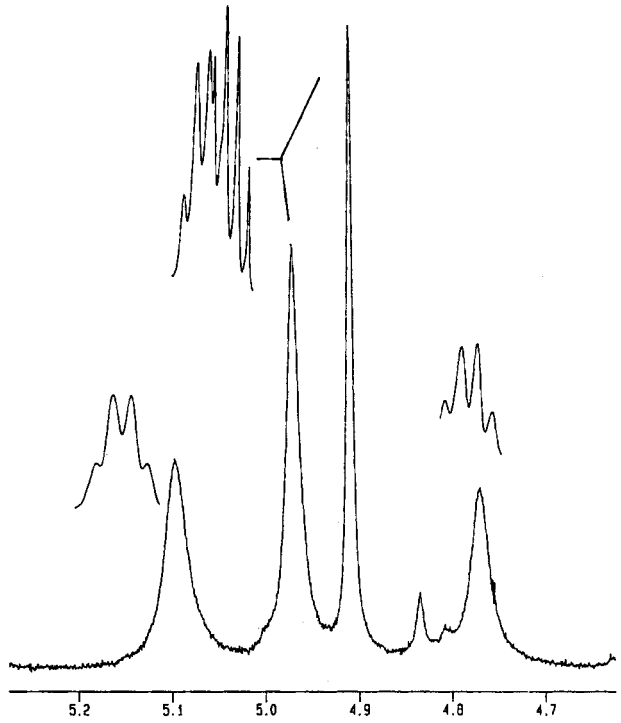

Figure 5. ^{1}H NMR of $Q_8[H_2F_6NaVW_{17}O_{56}]$ in CD_3CN. Insets: coupled $^{1}H\{^{19}F\}$ peaks.

purity of $[H_2F_6NaV^{V}W_{17}O_{56}]^{8-}$ which appears to be greater than 95%. The non-decoupled $^{1}H\{^{19}F\}$ spectra, Figure 5 insets, show that each of the four peaks can be resolved as a quartet (for the peaks at 5.09 and 4.77 ppm this is clearer by Gaussian apodization). The coupling constants, $^{1}J_{HF}$, are 10.7, 9.5, 10.4, and 10.8 Hz, respectively. The observation of quartets is consistent with protons adjacent to three fluorine atoms within F_3HO tetrahedra. In addition, the observation of four peaks indicates the presence of two isomers of $[H_2F_6NaV^{V}W_{17}O_{56}]^{8-}$. Thus, substitution of vanadium in a belt or capped position will each yield a nonsymmetric molecule with two different chemical shifts for the protons. The area ratios would seem to indicate that the peaks at 4.91 and 4.77 ppm are to be associated with the less abundant, probably capped substitution, while the peaks 5.09 and 4.97 are to be associated with the more abundant, probably belt substitution. This assignment is based only on probabilities. Importantly, the peak area ratios observed in the ^{1}H NMR are similar to those observed in the ^{51}V NMR and strongly support a conclusion for formation of both belt and capped vanadium-substituted $[H_2F_6NaV^{V}W_{17}O_{56}]^{8-}$. The poorer resolution of the quartets at 5.09 and 4.77 ppm versus the quartets at 4.97 and 4.91 ppm is associated with the proximity of ^{51}V ($I = {}^{7}/_{2}$) to the HF_3O tetrahedra for the former which broaden the peaks. The better resolved quartets are related to the distal (from vanadium) HF_3O tetrahedra. Note that ^{183}W ($I = {}^{1}/_{2}$) is not expected to cause significant peak broadening.

The $^{183}W\{^{19}F\}$ NMR of $[H_2F_6NaV^{V}W_{17}O_{56}]^{8-}$ as the lithium salt is very different from the ^{183}W NMR of the analogous but symmetric $[H_2F_6NaW_{18}O_{56}]^{7-}$ and underlines its nonsymmetric structure.[9] The ^{183}W NMR of the latter compound has narrow singlet at -141 ppm attributed to tungsten in the capped position and a broader doublet, due to fluorine coupling, at -153.6 and -157.3 ppm attributed to tungsten in the belt position. In this case, for $[H_2F_6NaV^{V}W_{17}O_{56}]^{8-}$, approximately 30 major peaks between -82 and -210 ppm ($NaWO_4$ reference) are observed along with numerous other minor peaks associated with W−W satellites, Figure 6. No further attempts were made to resolve the spectrum due to the lack of technical capability needed to carry out the required flourine decoupling experiment.[16]

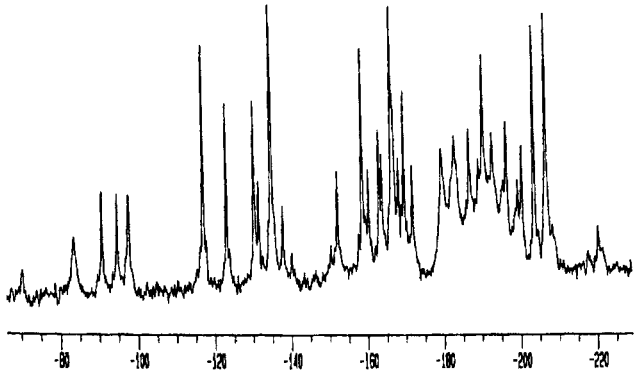

Figure 6. ^{183}W NMR of $K_8[H_2F_6NaVW_{17}O_{56}]$ in D_2O.

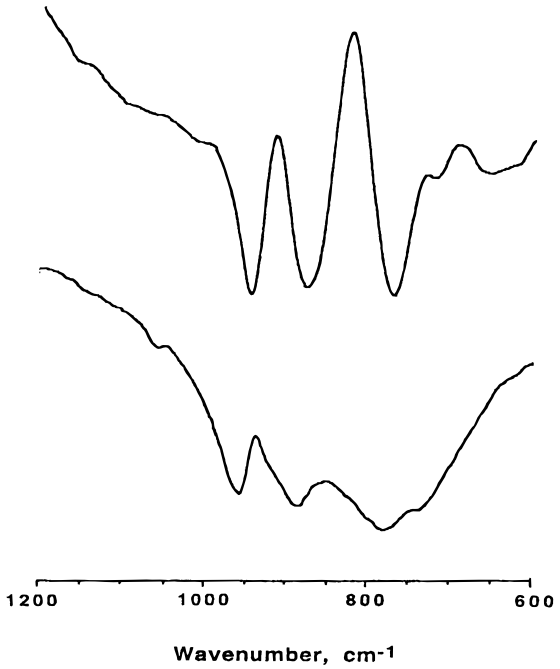

Figure 7. IR spectra of vanadium-substituted PFOMs. Bottom: $K_8[H_2F_6NaVW_{17}O_{56}]$ in KBr. Top: mixture of Keggin-type vanadium-substituted PFOMs.

The $[H_2F_6NaV^{V}W_{17}O_{56}]^{8-}$ polyfluorooxometalate was further characterized by UV−vis, IR, Figure 7, bottom, and cyclic voltammetry. The UV−vis of $[H_2F_6NaV^{V}W_{17}O_{56}]^{8-}$ in H_2O showed a maximum at 262 nm with $\epsilon \approx 34000$. Before oxidation with peroxydisulfate the crude purple $[H_2F_6NaV^{IV}W_{17}O_{56}]^{9-}$ showed an additional broad peak with a maximum at 422 nm. The IR spectrum was as generally expected for polyoxometalates and showed three peaks at 957, 887, and 780 cm^{-1} attributable to terminal, W−O_t, corner-sharing, W−O_c−W, and edge-sharing, W−O_e−W, functionalities, respectively. Importantly, this spectrum showed different absorption wavelengths compared to the spectrum of a Keggin-type PFOM (see Figure 7, top, and discussion below). The cyclic voltagram was clean, showing that the compound was of high purity. The oxidation wave for V^{IV}/V^{V} was at $+0.18$ V versus SCE, showing that the vanadium(V) state may be easily accessible under aerobic conditions.

(16) Each W peak is expected to appear as a triplet; this together with probable overlap of peaks makes assignments practically impossible without F decoupling.

Table 3. Crystallographic Data for the Keggin Polyfluorooxometalate Mixture[a]

space group	$P\bar{4}3m$
a, Å	11.162(3)
V, Å^3	1390.7(5)
z	1
ρ_{cald}, g cm^{-3}	3.63
μ(Mo Kα), cm^{-1}	237.32
no. of unique reflns	296
no. of reflns with $I \geq 3\sigma_I$	260
R (R_w)	0.044 (0.062)

[a] The structure was refined for a 1:1 mixture of $[(WO_3F)(V^{IV}W_{11}O_{36})]^{3-}$ and $[(H_2F_4)(V^{IV}W_{11}O_{36})]^{4-}$.

Characterization of the Vanadium-Substituted Keggin-Type Polyfluorooxometalates. The structure of the purple-black cubic crystals formed by recrystallization of the originally formed $[H_2F_6NaV^{IV}W_{17}O_{56}]^{9-}$ compound was pursued by various methods including X-ray diffraction, IR, ESR, and HPLC separation. The X-ray structure of the crystals formed, Table 3, was completely consistent with the structure of a Keggin-type compound. Importantly, however, the electron density at the central heteroatom position was not consistent with any cation or metal used in the synthesis. Rather, the electron density was typical of an atom of the second row of transition metals. Since no such metals were used in the synthesis, it is clearly suggested that the crystals should be a mixture of Keggin-type compounds with tungsten as well as protons, sodium and proton, or vanadium in the heteroatom position. On the basis of electron density and anionic charge (see below), the structure was *arbitrarily* refined for a 1:1 mixture of $[(WO_3F)(V^{IV}W_{11}O_{36})]^{3-}$and $[(H_2F_4)(V^{IV}W_{11}O_{36})]^{4-}$. Analysis by IR, Figure 7, top, clearly supports the conclusion that this mixture is structurally distinguishable from the quasi Wells−Dawson compound described above. Major peaks at 944, 884, and 768 cm^{-1} are attributable to terminal, W−O_t, corner-sharing, W−O_c−W, and edge-sharing, W−O_e−W, functionalities and are consistent with Keggin-type polyfluorooxometalates mentioned in the literature.[7−10]

The Keggin-type PFOM mixture was also analyzed by chromatography using HPLC to effect separation based on anionic charge.[17] Therefore, on a reversed-phase column, using a methanol:water eluent containing 50 mM *n*-butylamine and 20 mM citric acid, the HPLC showed that there were species of two different charges in an approximately 40:60 ratio in the mixture (retention times were 7.2 and 7.9 min, see the Experimental Section for more details). The mol ratio between charged species was not calibrated because the absorption coefficients are unknown. A further ESR spectrum of the Keggin PFOM mixture (all vanadium-containing compounds are expected to be ESR active), Figure 8, also showed the presence of two different V^{IV}-containing polyoxometalates. In an anisotropic solid state spectrum such as this, when vanadium(IV) is in a tetragonally distorted octahedral environment, two groups of lines for fields parallel and perpendicular to the V−O_t axis are observed.[18] For this mixture, for the field parallel to the V−O_t axis, it is easy to distinguish between two sets of eight lines, each with $A_{||}$ 185 G, associated with $g_{||} = 2.135$ for one compound and $g_{||} = 2.104$ for a second compound. Only one set of lines was observed for $g_{\perp}$. Thus, the X-ray analysis, HPLC separation, and ESR spectrum clearly revealed that upon recrystallization of $[H_2F_6NaV^{IV}W_{17}O_{56}]^{9-}$ at least two different polyfluorooxometalates of the Keggin structure were formed. Further analysis, after oxidation to vanadium(V) species with $S_2O_8^{2-}$, by ^{19}F NMR and ^{51}V NMR yielded clean spectra[19] but did not enable an unambiguous definition of the mixture.

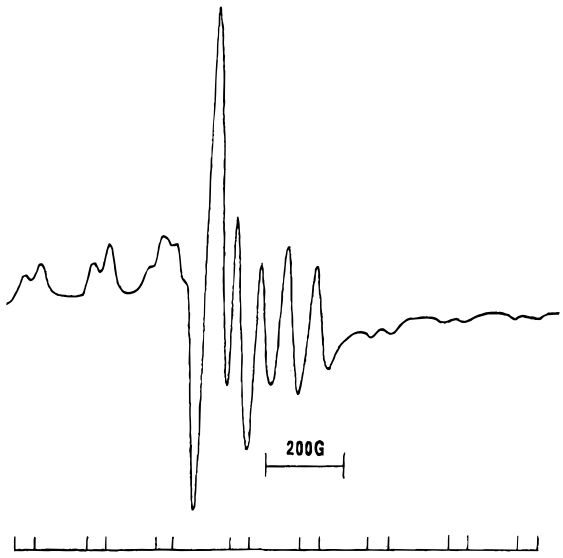

Figure 8. ESR spectrum of mixture of Keggin-type vanadium-substituted PFOMs. The two sets of eight peaks for $g_{||}$ are marked on the spectrum.

Table 4. Aerobic Oxidation of Alkyl Aromatic Compounds Catalyzed by Vanadium-Substituted PFOMs

Substrate	TON[a]	Products, mol%[b]
	3750	51% 46% 3%
	650	14% 86%
	700	10% 76% 9%
	1150	100%
	0	no reaction
	0	no reaction
	1250	55% 45%
	2300	93% 7%

Reaction Conditions: 100 mmol substrate, 0.02 mmol $K_8[H_2F_6NaVW_{17}O_{56}]$ in 10 mL acetate buffer (pH - 5.0), 120 °C, 5 atm O_2, 18 h. (a) mol all products/mol catalyst, (b) product selectivity.

Aerobic Oxidation of Alkyl Aromatic Compounds. The catalytic activity of the vanadium-substituted PFOMs was tested in the aerobic oxidation of alkyl aromatic compounds. A biphasic reaction system[20] was used whereby $K_8H_2F_6NaV^{V}W_{17}O_{56}$ dissolved in water was reacted with a neat alkyl aromatic compound at 120 °C under 5 atm of molecular oxygen in an autoclave. From the results shown in Table 4, one may observe that catalytic activity for oxidation at a tertiary benzylic position as in cumene was higher than catalytic activity at a secondary benzylic position, for example in ethylbenzene and isobutyl-

(17) Kirk, A. D.; Riske, W.; Lyon, D. K.; Rapko, B.; Finke, R. G. *Inorg. Chem.* **1989**, *28*, 792.

(18) Kuska, H. A.; Rogers, M. T. In *Radical Ions*; Kaiser, E. T., Kevan, L., Eds.; Interscience: New York, 1968; p 601.

(19) ^{19}F NMR: −159.1 (q, 1F), −161.8 (s, 0.9F), −162.2 (s, 1F), −163.8 (q, 0.9F), −164.0 (d, 0.3F), −164.2 (t, 1F), −165.5 (q, 0.9F). ^{51}V NMR: −503 ($\Delta\nu_{1/2} = 2500$ Hz), −513 ($\Delta\nu_{1/2} = 230$ Hz), −553 ($\Delta\nu_{1/2} = 710$ Hz)

(20) Such reaction systems are highly attractive from a technological point of view in that these biphasic systems allow for easy catalyst recovery and reaction workup. Cf.: Cornils, B.; Wiebus, E. *Chemtech* **1995**, 33.

Scheme 2

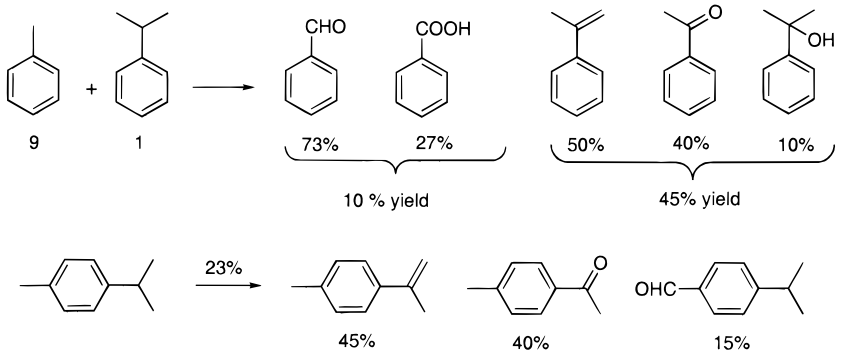

benzene, while primary benzylic compounds, toluene and 4-methoxytoluene, were inert. Cyclic alkyl aromatics such as 1,2,3,4-tetrahydronaphthalene and 9,10-dihydroanthracene were more reactive than acyclic compounds. In general concerning reaction selectivity, both oxidative dehydrogenation and oxidation at the benzylic position were observed. For cyclic alkyl aromatic compounds, there was mostly, 92−100%, oxidative dehydrogenation.[21] In cumene oxidation, dehydrogenation was accompanied by oxygenation mostly to ketone with significant methyl group cleavage. For acyclic compounds with secondary benzylic carbons, oxygenation to a ketone/alcohol mixture was dominant with some oxydehydrogenation. Although toluene alone did not react, the presence of a tertiary isopropyl moiety led also to oxidation at the primary position. Thus, oxidation of a 9:1 mixture of toluene and cumene yielded mostly benzaldehyde and benzoic acid and oxidation of *p*-cymene led to oxidation at both alkyl positions, Scheme 2. These latter experiments indicate that the oxygenation reactions are probably free radical autoxidations.[22] The vanadium-substituted PFOM selectively initiates formation of a benzylic radical (tertiary > secondary ≫ primary). Chain propagation via an intermediate alkylperoxo species is less selective, and primary benzylic radicals may therefore be formed in the presence of a compound with a tertiary (or secondary) benzylic carbon. The oxydehydrogenation, most common with vanadium-based compounds,[23] is hypothesized to be a result of electron and proton abstraction by the PFOM, to yield a PFOM−substrate complex,[5i,j] rather than a free radical. Subsequent and additional electron and proton abstraction yields the product and reduced PFOM. The latter is reoxidized by molecular oxygen. The autoxidation versus oxidative dehydrogenation pathway in the oxidation of cumene was tested as a function of the oxygen pressure and reaction temperature. As shown in Table 4, the oxygenation/dehydrogenation product ratio at 5 atm (120 °C) was ∼1:1 at 75% conversion. A decrease in the O_2 pressure to 1 atm led to selective, >98%, oxydehydrogenation although the conversion decreased significantly to 8.5% (425 turnovers). The effect of the reaction temperature was more complex, Table 5. One can note several trends. Catalytic activity was maximum at 90−120 °C with lower activity at high (150 °C) and much lower activity at 50 °C. Oxydehydrogenation was maximum at 90 °C and minimal at 150 °C. For autoxidation, lower temperatures favored cumyl alcohol formation whereas high temperatures favored acetophenone formation.

Table 5. Cumene Oxidation as a Function of Reaction Temperature

Temperature	Conversion, mol% (TON)	Product, mol%		
150 °C	34 (1700)	3	97	---
120 °C	75 (3750)	51	46	3
90 °C	78 (3900)	75	18	7
50 °C[a]	20 (1000)	50	5	45

Reaction conditions: 100 mmol cumene, 0.02 mmol $K_8[H_2F_6NaVW_{17}O_{56}]$ in 10 mL acetate buffer (pH - 5.0), 5 atm O_2, 18 h. (a) 64 h

Conclusions

The major findings of the research in this work are as follows.

(1) Mixed-addenda vanadium-substituted polyfluorooxometalates have been prepared, with two major species being formed: (a) a well-defined quasi Wells−Dawson type compound, $[H_2F_6NaV^VW_{17}O_{56}]^{8-}$, and (b) a mixture of Keggin-type compounds. The quasi Wells−Dawson type compound is significantly more stable for the vanadium(V) as opposed to vanadium(IV).

(2) According to ^{1}H, ^{19}F, and ^{51}V NMR analysis, it is concluded that vanadium is isomorphically substituted in both the belt and capped positions of $[H_2F_6NaV^VW_{17}O_{56}]^{8-}$.

(3) The $[H_2F_6NaV^VW_{17}O_{56}]^{8-}$ is catalytically active for the aerobic oxidation of alkyl aromatic compounds in biphasic (water-catalyst and substrate) media. Depending on the substrate reaction conditions (temperature and oxygen pressure) both autoxidation and oxydehydrogenation pathways were possible.

Experimental Section

Materials and Instruments. Reactants and solvents were all from commercial sources and were used without additional purification. Water was determined by thermogravimetric analysis (Mettler 50). ^{19}F NMR and ^{1}H NMR were measured on a Bruker 400 DRX instrument at 376.499 and 400.132 MHz in D_2O or CD_3CN using neat CF_3COOH as external standard. ^{51}V NMR and ^{183}W NMR were measured on a Bruker 300 AMX spectrometer at 78.86 and 12.505 MHz in D_2O using $VOCl_3$ and $NaWO_4$ as external standards. IR spectra were measured on a Nicolet 510M FT spectrometer; UV−vis spectra were taken on a HP 8452 diode array spectrometer; ESR spectra were measured at −120 °C using a Varian E-12 instrument. HPLC measurements were carried out on a Merck-Hitachi L6200, using 50 mM *n*-$BuNH_2$, 20 mM citric acid in 2:1 methanol−water adjusted to pH − 6.5 by NH_4OH as eluent. A reverse phase C_{18}, 4 × 250 mm, column was used with a flow rate of 0.5 mL/min; peaks were detected by UV at 240 nm. Oxidation reaction products were characterized using reference compounds when available by use of GLC (Hewlett-Packard 5890 gas chromatograph)

(21) Reactions carried out with the prototypical cobalt acetate catalyst (100 mmol of substrate, 0.02 mmol of $Co(OAc)_2 \cdot H_2O$ in 10 mL of acetate buffer (pH 5.0), 120 °C, 5 atm of O_2) showed a prevalence for oxygenation versus dehydrogenation. For example, tetralin yielded 73% tetralone and 27% naphthalene and dihydronaphthalene while cumene gave 83% acetophenone, 11% α-methylstyrene, and 6% cumyl alcohol. Total product yields were 50−60% higher.

(22) Sheldon, R. A.; Kochi, J. K. *Metal Catalyzed Oxidations of Organic Compounds*; Academic Press: New York, 1981.

(23) Cavani, F.; Trifirò, F. *Catal. Today* **1997**, *36*, 431.

with a flame ionization detector and a 15 m × 0.32 mm 5% phenylmethylsilicone (0.25 μm coating) capillary column and helium carrier gas. Products whose initial identity was questionable were unambiguously identified using a gas chromatograph equipped with a mass selective detector (GC-MS Hewlett-Packard GCD) equipped with the same column described above.

Synthesis. The zinc-substituted quasi Wells−Dawson type polyfluorooxometalate, $[ZnH_2F_6NaW_{17}O_{55}]^{9-}$ was synthesized according to the literature procedure.[10] Thus, 44 g of $NaWO_4 \cdot H_2O$ was dissolved in 100 mL of water in a Teflon beaker and brought to 80 °C. HF (49%) was added dropwise until the pH became 4.5. The white precipitate was filtered off, and the filtrate was reheated to 80 °C. Seven grams of $Zn(OOCCH_3)_2 \cdot H_2O$ dissolved in 5 mL of water was added slowly while the pH was kept at 4.5. The solution was stirred for an additional hour at 80 °C and cooled followed by the addition of 3 g of KCl. The white precipitate was filtered and recrystallized twice from water, yield 9.6 g. ^{19}F NMR in H_2O with neat CF_3COOH as standard: −140.3 (1), −160.1 (1), −162.5 (1), −165.8 (2.5), −168.7 (1) ppm (intensity).

The vanadium(V)-substituted Wells−Dawson type polyfluorooxometalate, $K_8[H_2F_6NaVW_{17}O_{56}] \cdot 7H_2O$, was synthesized by metathetical substitution of the zinc precursor using $VOSO_4$. In this way, 0.326 g (2 mmol) of $VOSO_4$ dissolved in 5 mL of an acetate buffer (pH = 5) was added over a period of 5 min to a solution of 4.8 g (1 mmol) of $[ZnH_2F_6NaW_{17}O_{55}]^{9-}$ in 40 mL of an acetate buffer (pH = 5) at 50 °C. The solution turned purple immediately. After stirring for 30 min, the solution was cooled and filtered. To the filtrate was added a saturated KCl solution, and the precipitate formed was filtered. The precipitate (3.0 g) was dissolved in 15 mL water and heated to 90 °C followed by addition of 750 mg of $K_2S_2O_8$. Upon addition of the oxidant the color of the solution turned from deep purple-brown to yellow in 20 min. Cooling of the solution yielded only yellow needlelike crystals, $K_8[H_2F_6NaVW_{17}O_{56}] \cdot 7H_2O$, yield 2.4 g, which were recrystallized from water. Before oxidation by $K_2S_2O_8$, it was determined that there was one vanadium atom per molecule by titration with $KMnO_4$. Potassium and sodium were determined by atomic absorption, tungsten was determined gravimetrically, and the hydration state was estimated by thermogravimetric analysis as the quionolate. Anal. of $K_8[H_2F_6NaVW_{17}O_{56}] \cdot 7H_2O$: calcd (found), K, 6.48 (6.59); Na, 0.48 (<0.5; detected but precision limited do to sensitivity limitation); V, 1.05 (1.15); W, 64.70 (63.87); H_2O, 6.34 (6.29); F, 2.19 (2.36).

Recrystallization of the original precipitate after the metathetical exchange with $VOSO_4$ without peroxydisulfate oxidation yielded purple-black cubic crystals. Anal. of the crystals: K, 4.85; Na, not detected; V, 1.47; W, 67.21; H_2O, 7.32. For a 1:1 mixture of $K_3[(WO_3F)(V^{IV}W_{11}O_{36})]$ and $K_4[(H_2F_4)(V^{IV}W_{11}O_{36})]$ with 26 water molecules by thermogravimetry one would expect K, 4.30; V, 1.60; W, 66.39; H_2O, 7.35. $Q_8[H_2F_6NaVW_{17}O_{56}]$ ($Q = (C_4H_9)_4N^+$) was prepared by adding 1 g (0.20 mmol) of $K_8[H_2F_6NaVW_{17}O_{56}] \cdot 7H_2O$ dissolved in 10 mL of water to 20 mL of water containing 5 g (15 mmol) of $(C_4H_9)_4NBr$. The yellow precipitate which formed immediately was filtered, washed with water, and dried under vacuum. Anal. Calcd (found): C, 25.00 (25.21); H, 4.72 (4.61); N, 1.82 (1.61); Na, 0.36 (less than limit of accurate detection); V, 0.83 (less than limit of accurate detection); W, 50.81 (52.02).

X-ray Analysis. Data were measured on a PW1100/20 Phillips four-circle diffractometer. Mo Kα ($\lambda = 0.71069$ Å) radiation with a graphite crystal monochromator in the incident beam was used. The unit cells were obtained by a least-squares fit of 24 centered reflections in the range $11° \le \theta \le 14°$ ($K_8[VH_2F_6NaW_{17}O_{56}] \cdot 7H_2O$) and $13° \le \theta \le 15°$ (Keggin V-PFOM). Intensity data were collected using the $\omega-2\theta$ method to a maximum 2θ of 50°. The scan width, $\Delta\omega$, for each reflection was $1.00 + 0.035 \tan\theta$ with a scan speed of 3.0 deg/min. Background measurements were made for a total of 10 s at both limits of each scan. Three standard reflections were measured every 60 min, and no systematic variations were observed. Intensities were corrected for Lorentz, polarization, and absorption effects. All non-hydrogen atoms were found using the results of the SHELXS-86 direct method analysis. The tungsten atoms were refined assuming a random substitution of one vanadium atom, and the electron densities were adjusted accordingly. Refinement proceeded to convergence by minimizing $\Sigma w(|F_o| - |F_c|)^2$. A final difference Fourier synthesis map showed several peaks less than 2.3 e/Å^3 scattered about the unit cell without significant feature. The discrepancy indices are $R = \Sigma||F_o| - |F_c||/\Sigma|F_o|$ and $R_w = [\Sigma w(|F_o| - |F_c|)^2/\Sigma|F_o|^2]^{1/2}$.

Oxidation of Alkyl Aromatic Compounds. Aerobic oxidation of alkyl aromatic compounds was carried out in a 300 mL stainless steel stirred Parr autoclave, by loading a glass beaker with 20 μmol of $K_8[H_2F_6NaVW_{17}O_{56}] \cdot 7H_2O$ dissolved in 10 mL of acetate buffer (pH 5) and 100 mmol of substrate. The autoclave was pressurized to 5 atm of O_2, and the biphasic (no solvent) system was stirred and heated to 120 °C for 16 h. After cooling, the composition of the organic phase was directly analyzed by gas chromatography. The water phase, twice extracted with CH_2Cl_2, showed no evidence of organic material.

Acknowledgment. This research was supported by the Basic Research Foundation administered by the Israel Academy of Sciences and Humanities. Dr. Shmuel Cohen is warmly thanked for the X-ray structure determination. Most of the research described was carried out at the Casali Institute of Applied Chemistry, The Hebrew University of Jerusalem.

Supporting Information Available: Complete tables of final positional parameters and *B*(eq) and intramolecular bond distances and angles for $[H_2F_6NaVW_{17}O_{56}]^{8-}$. This material is available free of charge via the Internet at http://pubs.acs.org.

IC990606S